

# ICOOOL Simulation of 10-20 GeV FFAG with Quasi-Realistic End Fields

J.S.Berg, R.Fernow, S.Kahn, R.B.Palmer, D.Trbojevic

15/8/2003

Abstract

A non-scaling triplet 10-20 GeV FFAG is simulated using the tracking code ICOOOL. The simulation was done both with, and without quasi-realistic magnet ends. Aperture requirements and non-linear resonances are examined at a normalized acceptance of 30 pi mm.

## Contents

1	Introduction	2
2	Input parameters	2
3	ICOOOL Simulation	5
4	Required apertures and peak fields	7
5	Amplitude effect on phase slip	7
6	Non-linear resonances	7
6.1	Half integer resonance	7
6.2	x-y Mixing	11
6.3	Non-linear resonance	11
7	Conclusion	12
8	Appendix ICOOOL files	13

# 1 Introduction

Non-Scaling FFAAGs were first proposed by Carol Johnstone[1]. It was shown that a strongly focusing FODO ring could be designed with a momentum acceptance as large as a factor of 3. Dejan Trbojevic[2] introduced triplet designs that appear to be more isochronous and have smaller circumferences and apertures. This paper will present simulations of a 10 to 20 GeV triplet lattice.

Most simulations of such FFAAGs have been done using idealized hard edged magnetic fields and varying approximations to higher order effects. Only the study by Meot[3] included an approximation to the end fields, but even here the end fields used were required not to overlap with those of any neighboring magnet. At least in the case studied here, this would be a poor approximation. This study, using ICOOL[4] allows end fields to overlap. It does this by summing the axial fields of each magnet using a hyperbolic tangent expressions for the ends, and allowing overlap. The resulting axial fields are then Fourier analyzed and the fields at all locations derived from these Fourier components by ICOOL. The lattice is assumed to be strictly periodic, with no injection/extraction insertion, and no errors.

## 2 Input parameters

The study is based on a lattice proposed by Dejan Trbojevic with the parameters given in table 1.

	Len m	$B_o$ T	$G_o$ T/m
$g_{gap}$	1.0328		
Focus combined function magnet	.5	-3.4099	66.978
$g_{gap}$	.1672		
Defocus combined function magnet	1.5	5.814	-35.701
$g_{gap}$	.1672		
Focus combined function magnet	.5	-3.4099	66.978
$g_{gap}$	1.0328		

Table 1: Parameters of magnets as provided by Trbojevic

These parameters describe fields assumed to stop abruptly at the magnet ends. Such fields are non-Maxwellian and will not contain some non-linear effects that any real magnet will have. In addition, realistic ends will significantly change the average bending and focusing properties of the magnets. However, this hard edged assumption has been used in other simulations, and ICOOL can choose to use it. We thus first use ICOOL to simulate the lattice with the hard edged assumption, so that comparisons can be made with these other codes.

To give a more realistic drop off of the magnets, we will use the following hyperbolic tangent form. Such a drop off is Maxwellian, but only a crude approximation to what the ends of a real magnet might do. More sophisticated end fields will be tried later.

$$B = B_o \frac{B_{fac}}{2} \left( \frac{e^{(z-z_1)/\Gamma_B} - e^{-(z-z_1)/\Gamma_B}}{e^{(z-z_1)/\Gamma_B} + e^{-(z-z_1)/\Gamma_B}} - \frac{e^{(z-z_2)/\Gamma_B} - e^{-(z-z_2)/\Gamma_B}}{e^{(z-z_2)/\Gamma_B} + e^{-(z-z_2)/\Gamma_B}} \right)$$

where  $z_1$  is the z position of the magnet start and  $z_2$  is the position of the magnet end.  $B_o$  is the field taken from the hard end example.  $B_{fac}$  is a parameter used to modify the design when the soft ends are used.

A similar expression is used for the field gradient  $G$ , but in this, the fall off parameter  $\Gamma_G$  has a value a factor of two smaller.

$$\Gamma_G = \frac{\Gamma_B}{2}$$

The faster fall off for the gradients reflects the faster theoretical power fall off of a quad vs a dipole. The factors  $B_{fac}$  were chosen to give performance similar, but not identical to the hard edged case. The factors, and resulting maximum fields, used are given in table 2, below. The Fields are plotted in fig 1.

	Len m	$B_o$ T	$G_o$ T/m	Bfac	Gfac	$\Gamma_B$ m	$B_{max}$ T	$G_{max}$ T/m
gap	1.0328							
F magnet	.5	-3.4099	66.978	1.2	1	.2	-3.36	66.03
gap	.1672							
D magnet	1.5	5.814	-35.701	1.02	1	.2	5.92	-35.70
gap	.1672							
F magnet	.5	-3.4099	66.978	1.2	1	.2	-3.36	66.03
gap	1.0328							

Table 2: Modified parameters including end fields

The mean bending per cell is not quite the same in the two cases, so the number of cells and circumferences are a little different:

	hard ends	soft ends
cell	m	4.9
n cells		59
circ	m	289
		318

Table 3: parameters for each example

The field strengths as a function of length are Fourier analysed, yielding the coefficients given in table 4. Sextupole terms due to the z variation of the quadrupoles are derived automatically by ICOOL. Sextupole terms due to the coil end shapes were not included, but will be added in a later paper, when available.

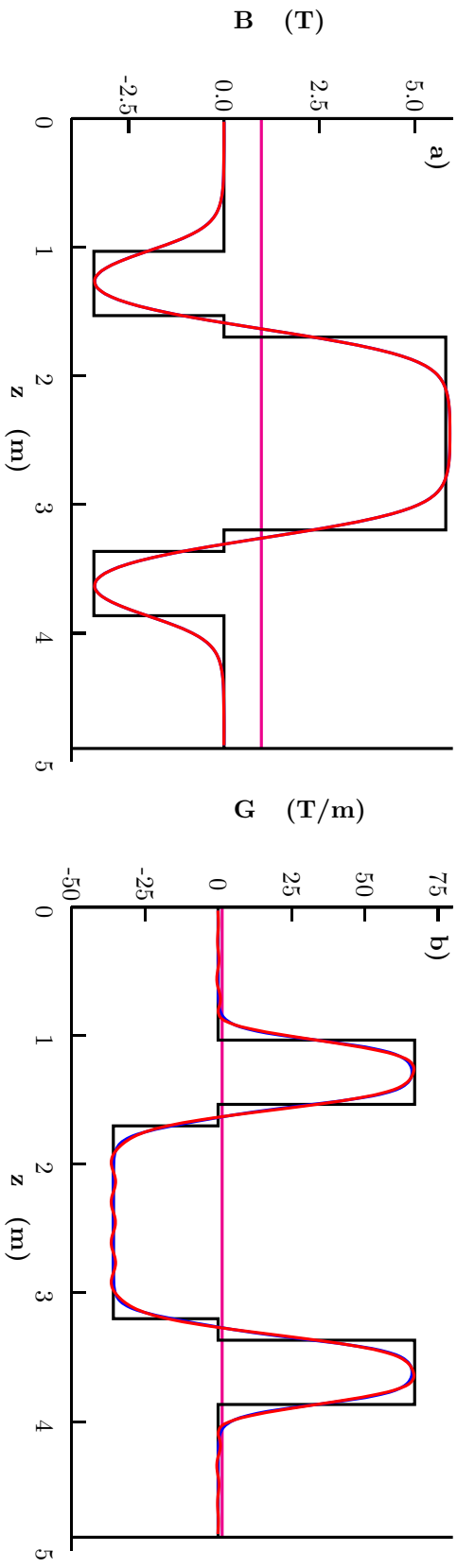


Figure 1: Shapes of a) hard edged fields (black), b) fields including tan end fields (blue), c) fields reproduced from 15 Fourier components (red).

i	$B(i)$ T	$G(i)$ T/m
0	.9803195	2.740101
1	-2.895885	16.53893
2	2.979532	-34.93562
3	-.5018952	6.650915
4	-1.210014	20.89505
5	.6177055	-9.08317
6	.1855154	-8.069601
7	-.1763015	4.489265

i	$B(i)$ T	$G(i)$ T/m
8	4.405256E-02	1.35215
9	-3.883789E-02	.1640327
10	-1.388343E-02	.458303
11	4.675247E-02	-1.96029
12	-7.055193E-03	-.5571176
13	-1.463328E-02	1.725461
14	1.062646E-03	.5901405
15	1.972909E-03	-1.068816

Table 4: Fourier components of bnding and gradient fields

The Fields and Gradients vs  $z$  for the hard edged example (black), the soft end example with tan fall offs (blue), and the fields from the Fourier approximation (red) are shown in Fig1. The blue trace is barely visible because the red Fourier approximation overlays it relatively well.

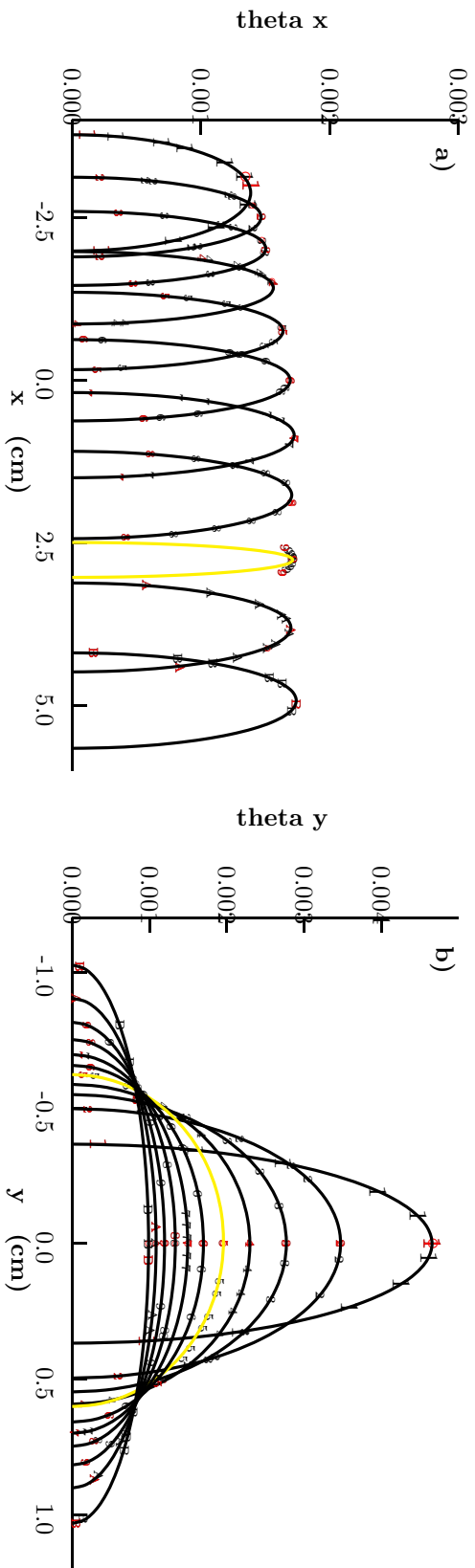


Figure 2: ICool phase plots using hyperbolic tangent ends, at ends of 20 cells, from small amplitude (emittance= $3\pi$  mm) tracks, injected with equal amplitudes in both x and y, with momenta in 1 GeV steps from 10 to 20 GeV. Fitted ellipses are shown as used to derive tunes, betas and orbit length. A yellow ellipse indicates a poor fit for which the data will not be used: a) in x, and b) in y

### 3 ICool Simulation

Off axis fields are derived, by ICool, from the axial fields and gradients given by the above Fourier approximation. One initial track per momentum was introduced at the midpoint of the long drift where it would be placed. The tracks were introduced on the axis, with differing transverse angles in x, y, or both. The tracks were then traced through a number of identical cells (typically 20).

For an initial study, the tracks were given small initial angles, with equal angles in the x and y planes. In each case the track positions were observed after each full cell, plotted on phase diagrams and fitted to ellipses: see fig.2. Yellow ellipses indicate a poor fit from which data will not be used. 11 Momenta were tracked in steps of 1 GeV/c from 10 to 20 GeV/c.

In fig.3 the closed orbit displacements, fitted beta functions, tunes, and closed orbit offsets are shown for both the hard edged and quasi-realistic cases.

The ICool data files are given in the appendix.

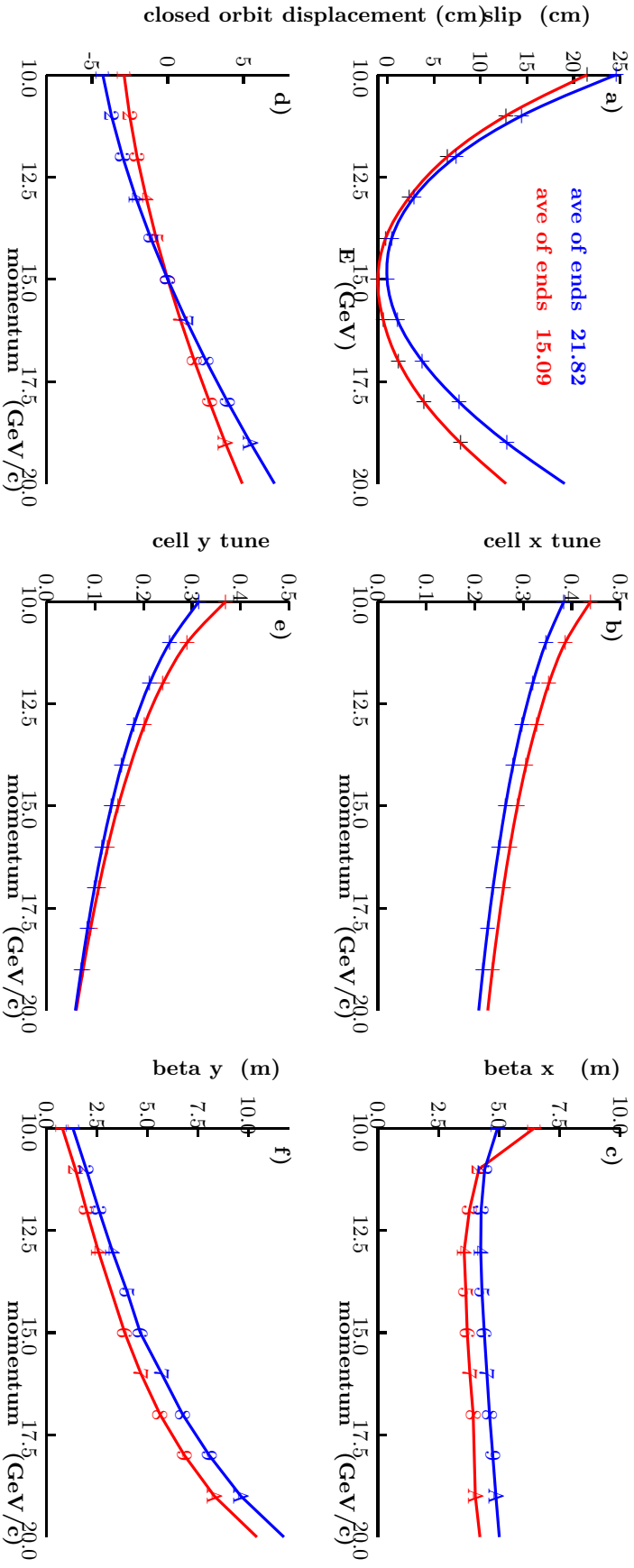


Figure 3: Parameters as a function of momentum for the hard edged example (blue) and hyperbolic tangent edged example (red): a) differences in orbit per revolution, b) x tune per cell, c) beta x at center of rf, d) closed orbit displacement at center of rf, e) y tune per cell, f) beta y at center of rf straight.

## 4 Required apertures and peak fields

A second ICOOL run was made with output at several positions along each cell. For this run, three initial tracks were introduced: a) with amplitude in x and none in y, b) the same amplitude in y and none in x, and c)  $1/\sqrt{2}$  of these amplitudes in both x and y simultaneously. The amplitudes corresponded to the required  $30 \pi$  mm acceptance.

The track positions are plotted in fig.4 at the center of the rf, at the centers of each magnet, and at the end of the longer defocus combined function magnet. Circles and ellipses are drawn that contain all tracks. A second larger circle and/or ellipse indicates plausible coil inside dimensions, assuming that a 30% aperture increment is needed to assure adequate field quality.

The tracks started with no y component (blue) remain in the mid plane as expected. Those with amplitudes in x and y paint a rectangular pattern. Those injected with only amplitude in the y direction remain mostly in that plane, but do have some significant coupling as seen by a widening of the patterns, as will be discussed in section 6.

The peak fields on the insides of the coils can be extracted by reading the vertical field at the radius of the larger circles or ellipses. The peak field values are also given in the figure. The peak field in the defocus combined function magnet is seen to be about 1 T less (7.7 vs 8.7 T), if the magnets are elliptical instead of circular. This could make a significant difference in cost since it may allow 4.2 deg and NfTi conductor, instead of 2 deg or NbSn.

## 5 Amplitude effect on phase slip

As in the initial runs, ICOOL was run with outputs only at the end of each cell, for 20 cells, but the initial tracks were given larger transverse momenta, corresponding to acceptances of 30 pi mm. Three tracks were started at each momentum: 1) with initial angle in y, 2) but none in x; and 3) initial angle in x, but not in y; and equal angles in x and y (but  $\sqrt{2}$  of those in x or y alone). As before, runs were made with 11 initial momenta, spaced by 1 GeV/c. The total time to propagate each track was determined, divided by the number of cells tracked, and multiplied by the number of cells in the ring (65). These results are compared with those for small amplitude tracks.

Fig.5 shows that there is a significant increase in the orbit lengths for large amplitude tracks at low momenta, but a negligible effect at high momenta. The effect is greater for motion in the y direction than in the x direction. Clearly, one dimensional studies of longitudinal motion will not give accurate results. In a later paper, we will add acceleration and study the longitudinal motion including transverse effects.

## 6 Non-linear resonances

The strongest non-linear effects were seen when tracks were started with large amplitude (corresponding to 30 pi mm) in y, but no amplitude in x. As before, runs were made with 11 initial momenta, spaced by 1 GeV/c, but, to search for resonances, the initial momenta were stepped by 0.05 GeV/c. Resonant effects were particularly apparent with an initial momentum of 9.85 GeV/c. Results from this run are shown in fig.6. Three different non-linear effects were observed.

### 6.1 Half integer resonance

Instability at 30 pi mm, is observed when the momentum is equal or lower than 9.6 GeV/c. This is due to the approach to the half integer tune. It is not shown in figure 6.

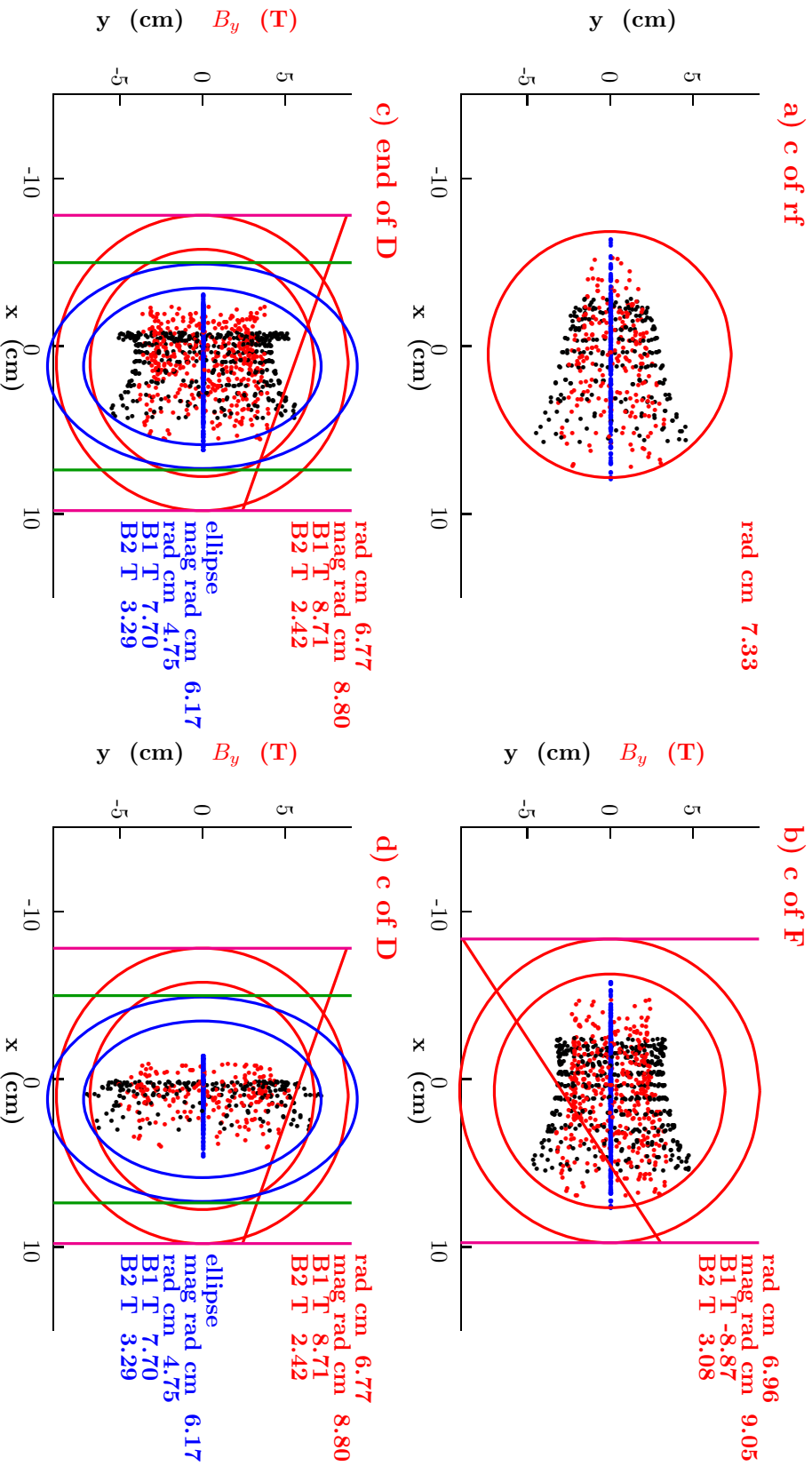


Figure 4: Magnetic fields vs.  $x$ , and track positions in  $x$  vs.  $y$  over 50 cells at the a) center of rf straight, b) center of focus combined function magnet, c) end of defocus combined function magnet, d) center of defocus combined function magnet. The circles indicate the required good field bounds and magnet coil inside dimensions.



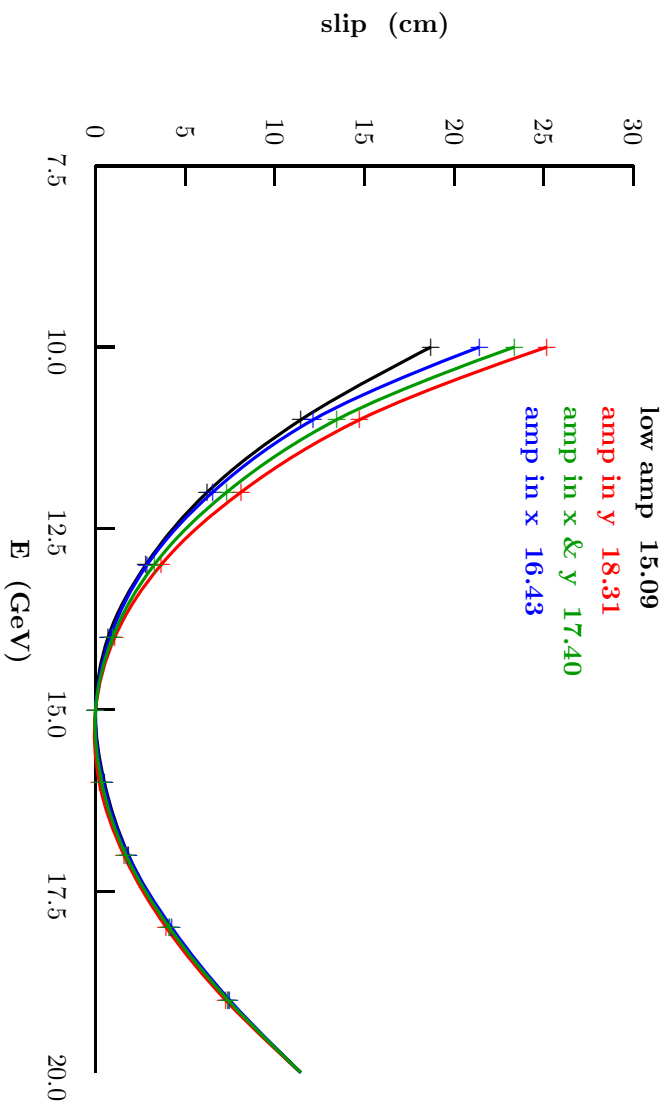


Figure 5: Differences in orbits around the ring for a) low amplitudes; b) 30 pi mm in y; c) 30 pi mm in x&y; d) 30 pi mm in x. The numbers given are averages of the max and min energies in cm.

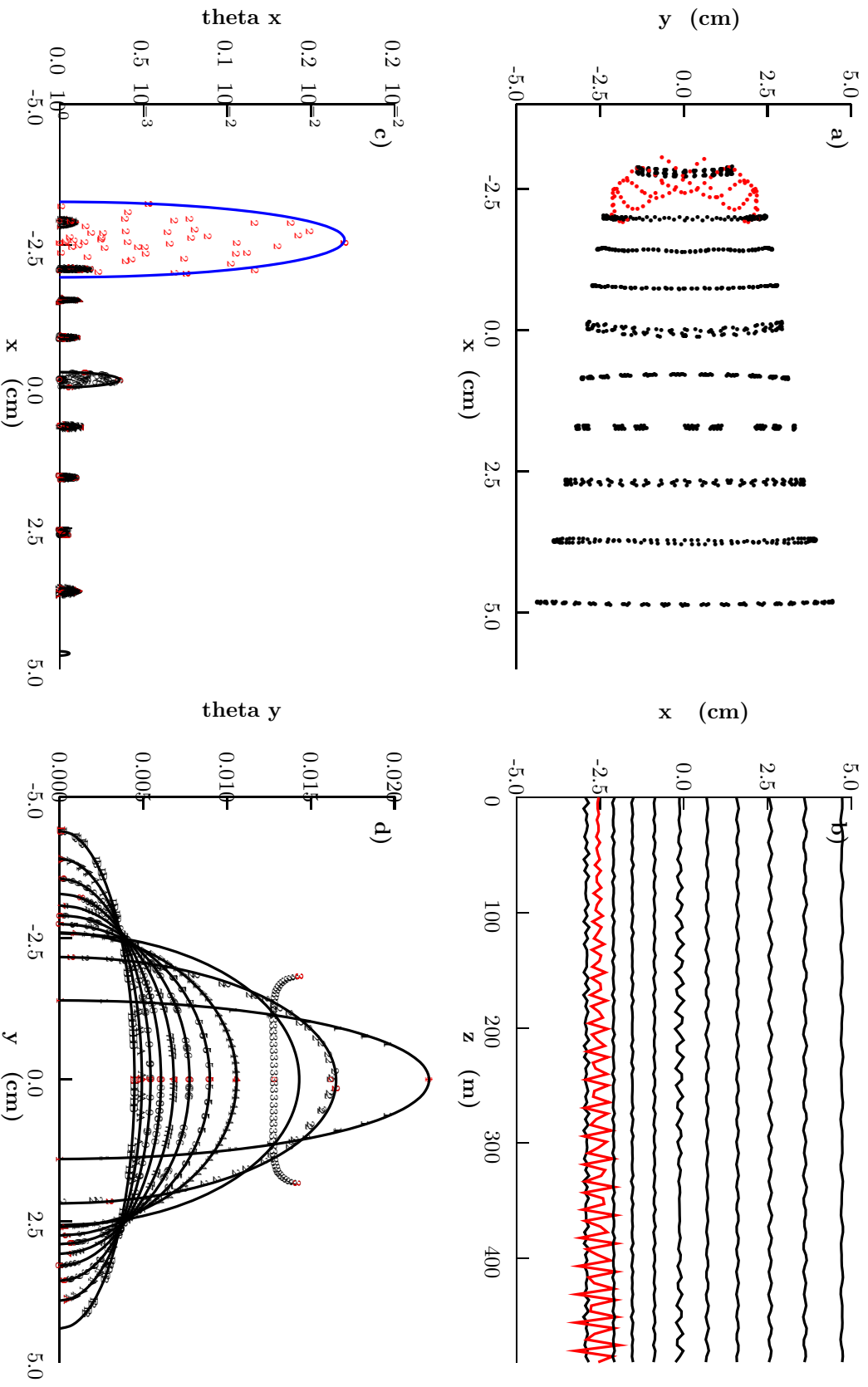


Figure 6: plots of motions at the center of the rf, of particles with 10 momenta (9.85 to 19.85 GeV in steps of 1 GeV), injected with large amplitude (30 pi mm), only in the y plane, tracked through 100 cells: a) x y positions at the center of the rf straightights, b) x positions vs z, c) phase plots in the x direction, d) phase plots in the y direction.

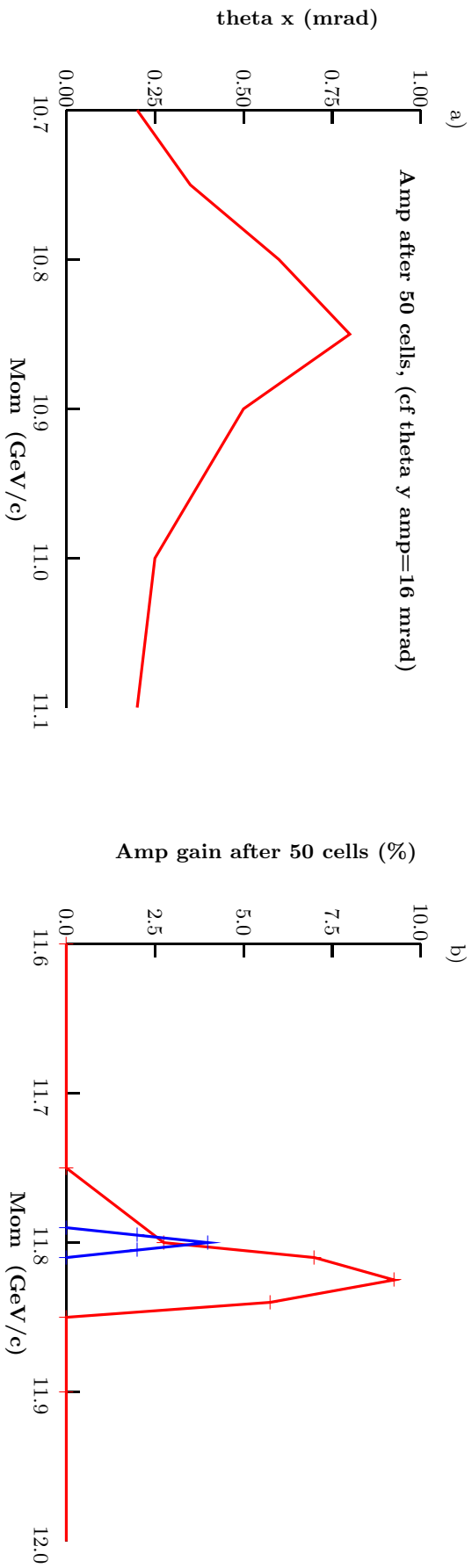


Figure 7: a) Induced amplitudes in x, from an initial amplitude in y, after 50 cells as a function of particle momentum for 30 pi mm in y; b) Amplitude y gain after 50 cells due to the  $y=0.25$  resonance in y vs particle energy, for 30 pi mm in x & y (red) and 30 pi mm in x & y (blue).

## 6.2 x-y Mixing

Fig. 6a shows the  $x, y$  positions at the end of each cell for 50 cells. It shows primarily vertical bands corresponding to the expected  $y$  motion, but in one case (10.85 GeV) the motion is seen to be greatly broadened in the  $x$  direction, indicating relatively strong  $x, y$  mixing and possible emittance growth.

The  $x, z$  plots in fig 6b show some coupling into this plane at many momenta, but such coupling results mostly in a beat, without any instability occurring. But at the specific momentum of 10.85 GeV/c, the amplitude continues to grow without apparent limit, indicating an instability

Fig 6c shows the  $x, p_x$  motion induced by the coupling from the  $y$  motion. Figure 6d will be referred to below.

Fig 7a shows that this  $x, y$  coupling resonance is narrow (approx 0.1 GeV), which, relative to the energy gain per turn (approx 1 GeV), should not be a problem;

Similar effects have already been reported by Meot[3], who also showed that this coupling is strongly amplitude dependent.

## 6.3 Non-linear resonance

At a  $y$  tune of .25 there is a non-linear resonance in  $y$  as seen in Fig 6d. Fig 7b shows that this  $y$  instability is even narrower (.05 GeV) than the coupling resonance, and its growth rate is slow enough (amplitude increase of about 10 percent after 50 cells), that it too should not be a problem.

A run with equal amplitudes in  $x$  and  $y$ , but both  $\sqrt{2}$  of those in  $x$  or  $y$  alone (corresponding to the same normalized 30 pi mm acceptance) showed an even narrower and weaker resonance at the  $y$  tune of 0.25 (see figure 7).

Resonances in  $y$  at a tune of 0.33 were searched for but not found. No resonances were seen at any tune for tracks only in the  $x$  direction.

## 7 Conclusion

This study has tracked an example of a triplet non-scaling FFAg, using quasi-realistic magnet end fields and all non-linear effects. Particles were tracked, without acceleration, at stepped momenta over a 2:1 momentum range (10-20 GeV/c). Several non-linear effects were observed at amplitudes corresponding to a transverse normalized acceptance of 30 pi mm, but none appeared large enough to cause significant emittance growth with acceleration over 20 turns. Further work can incorporate more realistic coil ends and include acceleration.

## References

- [1] C. Johnstone, W. Wan, and A. Garren. Fixed Field Circular Accelerator Design”, Proc 1999 Particle Accelerator Conference, New York, NY, March 29 1999, pp 3068.
- [2] Thbojevic; KEK Workshop July, 2003; [http://hadron.kek.jp/FFAG/FFAG03\\_HP/](http://hadron.kek.jp/FFAG/FFAG03_HP/)
- [3] Meot; KEK Workshop July, 2003; [http://hadron.kek.jp/FFAG/FFAG03\\_HP/](http://hadron.kek.jp/FFAG/FFAG03_HP/)
- [4] R. Fernow, <http://pubweb.bnl.gov/people/fernow/icool/>

## 8 Appendix ICOOL files

The simulation was done with ICOOL version 2.57, obtainable, together with the operating manual at <http://pubweb.bnl.gov/people/ferrow/icool/>. For the hard end case one needs the appropriate FOR001.DAT file plus the FOR003.DAT file. For the soft end case one needs the appropriate FOR001.DAT file plus the FOR003.DAT and the FOR056.DAT files.

### FOR001.DAT for Hard Edge Method

```

Dejan first ftag 30 pi mm (q4a)
$cont npart=100000 nsections=100 varstep=.false. nprint=-1 prlevel=3
ntuple=.false. rtuple=.false. rtuplen=1 output1=.true. phasemode1=3
fsav=.true. fsavset=.true. izfile=86 bgen=.false. DECTRK=.TRUE.$
 $ints ldecay=.true. declav=1 ldedx=.true. lstrag=.true. lscatter=.true.
delev=2 straglev=4 scatlev=4 $
 $nhs $ ! no histograms
 $nsc $ ! NO scatter plot
 $nzh $ ! no z-histories
 $nrh $ ! no r-histories
 $nem $ ! no 2-D emittance calculations
 $ncv $ ! no covariance calculations
SECTION
 ! start problem definition
REEP
 2 0.225 0. 0. 3
BEGS
SREGION          ! define a region          DRIFT 1M
1.0328 1 0.003   ! length, 1 radial subregion, step
1 0. .1          ! radial extent
NONE ! no associated field
0. 0. 0. 0. 0. 0. 0. 0. 0. 0. 0. 0. 0. 0. 0. 0. 0. 0. 0. 0.
VAC ! vacuum material
CBLOCK ! cylindrical block geometry
0. 0. 0. 0. 0. 0. 0. 0. 0. 0. 0. 0. 0. 0. 0. 0. 0. 0. 0. 0.
 ! OUTPUT
 ! OUTPUT
SREGION          ! define a region          DRIFT .5 m
.5 1 0.003       ! length, 1 radial subregion, step
1 0. .25         ! radial extent
DIP              ! DIPOLE defocus
1. -3.41 0 15 66.978 0. 0. 0. 0. 0. 0. 0. 0. 0. 0 0 ! mode By 0 p
VAC              ! vacuum material
CBLOCK          ! cylindrical block geometry
0. 0. 0. 0. 0. 0. 0. 0. 0. 0. 0. 0. 0. 0. 0. 0. 0. 0. 0. 0.
 ! OUTPUT
 ! OUTPUT
SREGION          ! define a region          DRIFT .5 m
.1672 1 0.003    ! length, 1 radial subregion, step

```

```

1 0. 1.0          ! radial extent
NONE ! no associated field
0. 0. 0. 0. 0. 0. 0. 0. 0. 0. 0. 0. 0. 0. 0. 0. 0. 0. 0. 0.
VAC ! vacuum material
CBLOCK ! cylindrical block geometry
0. 0. 0. 0. 0. 0. 0. 0. 0. 0. 0. 0. 0. 0. 0. 0. 0. 0. 0. 0.
! OUTPUT
SREGION          ! define a region          .5 m D
1.5 1 0.003      ! length, 1 radial subregion, step
1 0. .25         ! radial extent
DIP              ! DIPOLE defocus
1. 5.814 0 15 -35.701 0. 0. 0. 0. 0. 0. 0. 0. 0. 0. 0. 0. 0. 0. 0. 0. 0. 0.
VAC              ! vacuum material
CBLOCK          ! cylindrical block geometry
0. 0. 0. 0. 0. 0. 0. 0. 0. 0. 0. 0. 0. 0. 0. 0. 0. 0. 0. 0.
! OUTPUT
SREGION          ! define a region          DRIFT .5 m
.1672 1 0.003    ! length, 1 radial subregion, step
1 0. 1.0         ! radial extent
NONE ! no associated field
0. 0. 0. 0. 0. 0. 0. 0. 0. 0. 0. 0. 0. 0. 0. 0. 0. 0. 0. 0.
VAC ! vacuum material
CBLOCK ! cylindrical block geometry
0. 0. 0. 0. 0. 0. 0. 0. 0. 0. 0. 0. 0. 0. 0. 0. 0. 0. 0. 0.
! OUTPUT
SREGION          ! define a region          .3 m F
.5 1 0.003       ! length, 1 radial subregion, step
1 0. .25         ! radial extent
DIP              ! DIPOLE defocus
1. -3.41 0 15 66.978 0. 0. 0. 0. 0. 0. 0. 0. 0. 0. 0. 0. 0. 0. 0. 0. 0. 0.
VAC              ! vacuum material
CBLOCK          ! cylindrical block geometry
0. 0. 0. 0. 0. 0. 0. 0. 0. 0. 0. 0. 0. 0. 0. 0. 0. 0. 0. 0.
! OUTPUT
SREGION          ! define a region          DRIFT 1M
1.0328 1 0.003   ! length, 1 radial subregion, step
1 0. .1          ! radial extent
NONE ! no associated field
0. 0. 0. 0. 0. 0. 0. 0. 0. 0. 0. 0. 0. 0. 0. 0. 0. 0. 0. 0.
VAC ! vacuum material
CBLOCK ! cylindrical block geometry
0. 0. 0. 0. 0. 0. 0. 0. 0. 0. 0. 0. 0. 0. 0. 0. 0. 0. 0. 0.
ENDSECTION

```

# FOR001.DAT for soft end case

```

Dejan 10-20 fflag with ends y only (demo)
$cont npart=11 nsections=50 varstep=.false. nprint=-3 prlevel=1
ntuple=.false. rtuple=.false. output1=.true. phasemodel=3
fsav=.false. fsavset=.false. bgen=.false. $
$ints ldecay=.true. declav=1 ldedx=.true. lstrag=.true. lscatter=.true.
delev=2 straglev=4 scatlev=4 $
$hs $
$nc $
$nz $
$nrh nrhist=0 $
$nem nemit=2 pxycorr=.true. pzcorr=.true. bzfldprd=3.5 $
1 1322
$ncv ncover=2 $
1 1322
SECTION
REPP
2 15.0 0. 0. 3 ityp refp to grad0 mode (3=const p 4=with acc)
BEGS
=====
CELL i----- regular cell
1
.FALSE. i do not flip field sign between cells
BSOL i multipole field input
4. 56 15 3 0 1 1 1 1 1 1 1 1 1 0. imode file mom order 1/r scale-factors
i-----
OUTPUT
SREGION i define a region Drift rf center to F center
1.28 1 0.003 i length, 1 radial subregion, step
1 0. .1 i radial extent
NONE i no associated field
0. 0. 0. 0. 0. 0. 0. 0. 0. 0. 0. 0. 0. 0. 0.
VAC i vacuum material
CBLOCK i cylindrical block geometry
0. 0. 0. 0. 0. 0. 0. 0. 0. 0. 0. 0. 0. 0.
OUTPUT
SREGION i define a region Drift F center to D end
.42 1 0.003 i length, 1 radial subregion, step
1 0. .1 i radial extent
NONE i no associated field
0. 0. 0. 0. 0. 0. 0. 0. 0. 0. 0. 0. 0. 0. 0.
VAC i vacuum material
CBLOCK i cylindrical block geometry
0. 0. 0. 0. 0. 0. 0. 0. 0. 0. 0. 0. 0. 0. 0.
OUTPUT

```

```

SREGION
.75 1 0.003          ! define a region Drift D end to D center
1 0. .1              ! length, 1 radial subregion, step
                     ! radial extent
NONE ! no associated field
0. 0. 0. 0. 0. 0. 0. 0. 0. 0. 0. 0. 0. 0. 0. 0. 0. 0. 0. 0.
VAC ! vacuum material
CBLOCK ! cylindrical block geometry
0. 0. 0. 0. 0. 0. 0. 0. 0. 0. 0. 0. 0.
OUTPUT
SREGION
.75 1 0.003          ! define a region Drift D end to D center
1 0. .1              ! length, 1 radial subregion, step
                     ! radial extent
NONE ! no associated field
0. 0. 0. 0. 0. 0. 0. 0. 0. 0. 0. 0. 0. 0. 0. 0. 0. 0. 0. 0.
VAC ! vacuum material
CBLOCK ! cylindrical block geometry
0. 0. 0. 0. 0. 0. 0. 0. 0. 0. 0. 0. 0.
OUTPUT
SREGION
.42 1 0.003          ! define a region D end to F center
1 0. .1              ! length, 1 radial subregion, step
                     ! radial extent
NONE ! no associated field
0. 0. 0. 0. 0. 0. 0. 0. 0. 0. 0. 0. 0. 0. 0. 0. 0. 0. 0. 0.
VAC ! vacuum material
CBLOCK ! cylindrical block geometry
0. 0. 0. 0. 0. 0. 0. 0. 0. 0. 0. 0. 0.
OUTPUT
SREGION
1.28 1 0.003         ! define a region F center to rf center
1 0. .1              ! length, 1 radial subregion, step
                     ! radial extent
NONE ! no associated field
0. 0. 0. 0. 0. 0. 0. 0. 0. 0. 0. 0. 0. 0. 0. 0. 0. 0. 0. 0.
VAC ! vacuum material
CBLOCK ! cylindrical block geometry
0. 0. 0. 0. 0. 0. 0. 0. 0. 0. 0. 0. 0.
ENDCELL
ENDSECTION

```

### F003.DAT input tracks for either case

```

title
0 0 0 0 0 0 0 0
1 0 2 0 8.6667E-11 1.0
-3.1311E-02 0.0000E+00 0.0000E+00 5.9947E-02 2.0836E-01 9.9977E+00 0 0 0 0 0 0
2 0 2 0 8.6667E-11 1.0
-2.6844E-02 0.0000E+00 0.0000E+00 6.8911E-02 1.7093E-01 1.0999E+01 0 0 0 0 0 0

```



